Protein Crystallography at TPS

The fruitful results from protein crystallography (PX) that yielded six Nobel prizes in the past two decades have shown the importance of this technique. The major developments of advanced hardware and software have facilitated the entry of both academic and industrial researchers into this field. Nevertheless, when facing challenging projects related to viruses or membrane proteins, researchers must still overcome many experimental difficulties, such as crystals with large unit cells or small sizes, or both.

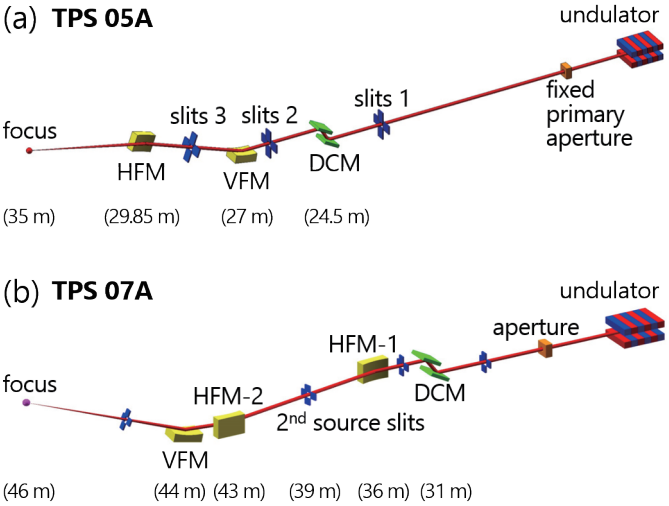

Fig. 1: Layout of beamlines (a) **TPS 05A** protein microcrystallography and (b) **TPS 07A** micro-focus protein crystallography.

The small divergence, small beam size and large flux-density features of protein micro-crystallography beamline **TPS 05A** offer an excellent opportunity for research with crystals of large unit cells. Generated by an IU22 undulator (length 3 m), with a double-crystal monochromator (DCM) cooled with liquid nitrogen and Kirkpatrick-Baez (K-B) mirrors (**Fig. 1(a)**), the beam properties at the sample position attain a beam size 65 × 36 μm^2 (H x V), energy range 5.7–20 keV (2.175–0.62 Å), beam divergence 500 × 100 μrad^2 (H x V), energy resolution ~2.2 × 10^{-4} and flux 1.0 × 10^{13} photons/s. Opened to users in 2017, **TPS 05A** has become a powerful tool for research on protein complexes and viruses that typically suffer from massive overlaps of diffraction spots caused by large unit cells. This issue can be solved when the diffraction data are collected at **TPS 05A** (**Fig. 2**).

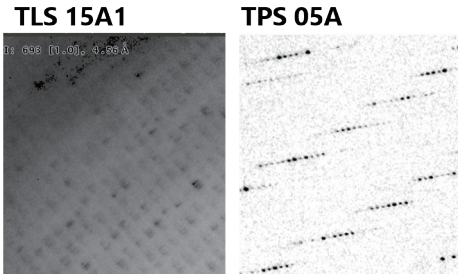

Fig. 2: Comparison of diffraction patterns between **TLS 15A1** (left) and **TPS 05A** (right).

To maintain a small divergence, the flux density of **TPS 05A** is compromised to be the same when selecting smaller beam sizes with apertures; this condition greatly affects the efficiency of raster scan and multi-crystal data collection for crystals of size a few micrometres. A micro-focus beamline, **TPS 07A**, for protein crystallography is hence currently under construction, to provide beam sizes from 30 to 1 microns. Using focusing instead of defining apertures, **TPS 07A** will be able to provide a higher flux density for much smaller beam sizes.

The main difference between **TPS 05A** and **TPS 07A** is the focusing method. On top of the Kirkpatrick-Baez (K-B) mirrors, **TPS 07A** adopts a two-stage focusing method in the horizontal direction on adding a first horizontal focusing mirror at 36 m and placing slits opening 2.5 microns as a secondary source (**Figs. 1(b) and 3**). The beam properties at the sample position are expected to include beam sizes 1.76 × 0.67 μm^2 (H x V), energy range 5.7–20 keV (2.175–0.62 Å), beam divergence 660 × 560 μrad^2 (H x V), energy resolution ~1.7 × 10^{-4} and flux 1.0 × 10^{12} photons/s for beam size 1 micron. Also, exploiting the greater divergence property, larger beam sizes up to 30 microns become achievable by adjusting the opening of secondary slits and moving the diffractometer downstream along the beam axis (**Fig. 4**).

To handle crystals with large unit cells, the endstation of **TPS 05A** is equipped with a detector (MX300HS) of high speed and large area, a diffractometer (MD2) of high speed and high precision, an automatic sample changer (ISARA), and an adjustment table of high loading and precision (**Fig. 5**). Under these conditions, users have now routinely used shutterless data collection. Not only is the efficiency of data collection increased but also the data quality is improved because the systemic errors from shutter jittering and rotation-axis synchronization are greatly decreased. At **TPS 05A**, only a few tens of seconds are required to collect a single data set.

Designed to treat tiny crystals in large amounts, the endstation of **TPS 07A** will be equipped with an even faster detector (Eiger 2X 16M), a diffractometer (MD3) of the greatest precision, an automatic sample changer (ISARA) and a precision adjustment table.

According to simulation, **TPS 07A** will be at third and fourth places worldwide in beam size and flux density, respectively. The time to the Henderson limit (*i.e.*, the duration of exposure that attains an X-ray dose at which the crystal diffraction power decreases by half) is 0.05 s, which falls behind only 0.004 s of MicroMAX, 0.017 s of FMX and 0.02 s of SP8 BL32XU (**Table 1**). The high flux density decreases the duration of data collection for tiny crystals, which increases the efficiency of data collection. That condition makes **TPS 07A** one of the first choices in Asia for research projects with tiny crystals.

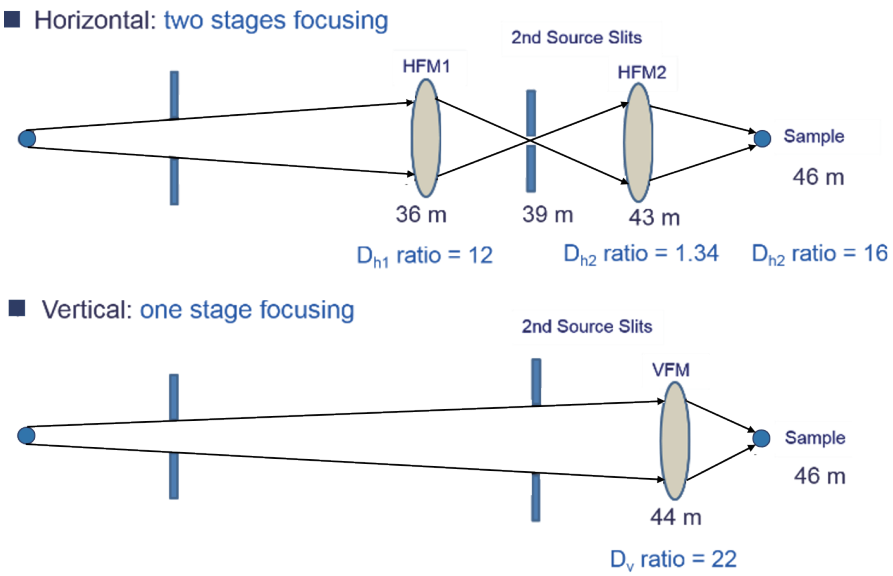

Fig. 3: Schematic diagram of two-stage focusing at **TPS 07A**.

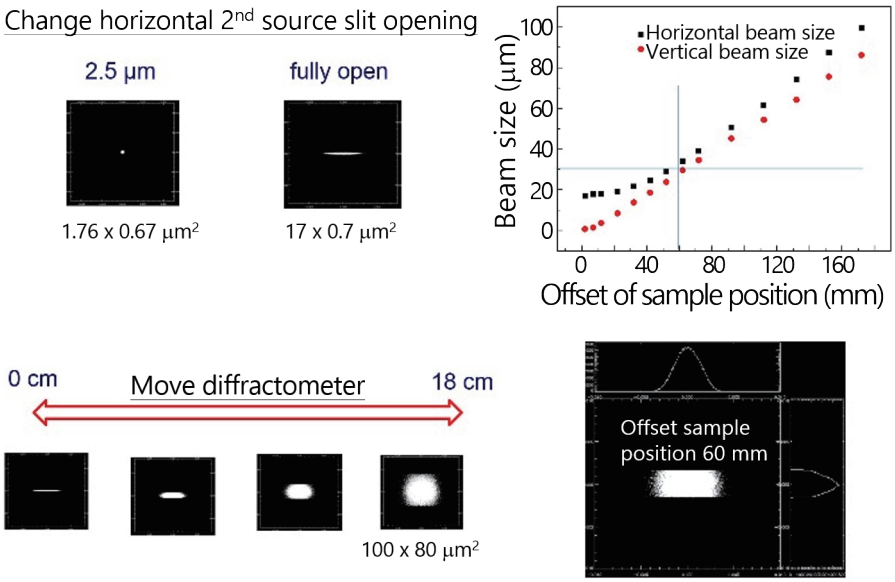

Fig. 4: Adjustable beam size of **TPS 07A**.

At both **TPS 05A** and **TPS 07A**, the smaller beam size, faster detector and high-speed precision diffractometers enable advanced methods of data collection, such as raster/grid scan and helical scan. Scanning with X-rays directly, the raster scan function could not only locate the crystal positions of crystals barely visible with an optical microscope but also probe for the region of best quality of inhomogeneous large crystals. For homogeneous large or needle-shaped crystals, the helical scan can make use of the entire crystal volume to mitigate the influences of radiation damage. With these methods, diffraction data are obtained of enhanced quality.

One must bear in mind that it is difficult to collect a complete data set from a crystal of size less than 10 microns because of radiation damage; an approach of multi-crystal data collection is hence required to address this problem. Both **TPS 05A** and **TPS 07A** provide new automatic sample changers that change samples within tens of seconds to increase the efficiency of data collection for many tiny crystals. More-

Fig. 5 Endstation of **TPS 05A**.

Table 1 Performance comparison of high-demagnification-ratio micro-focus PX facilities worldwide

	Energy range (keV)	Beam size (μm²) (H x V)	Flux density (ph s^{-1} $μm^{-2}$)	Henderson limit (s)
MAX IV/MicroMAX	5.0–30.0	1.0 × 1.0	1.0×10^{13}	0.004
NSLS II/FMX	5.0–30.0	1.0 x 1.5	2.3×10^{12}	0.017
SP8/BL32XU	9.0–15.0	1.0 x 1.0	2.0×10^{12}	0.02
NSRRC/TPS 07A	**5.7–20.0**	**1.76 × 0.67**	**8.5×10^{11}**	**0.05**
PETRA III/P14	6.0–20.0	5.0 × 10.0	2.0×10^{11}	0.2
SLS/X06SA	5.7–17.5	2.0 × 1.0	1.0×10^{11}	0.4
DLS/ID24	6.4–20.0	7.0 x 6.0	7.1×10^{10}	0.56
ESRF/ID23-2	14.2	10.0 x 4.0	6×10^{10}	0.67

Sources:
Max IV/MicroMAX: https://www.maxiv.lu.se/accelerators-beamlines/beamlines/micromax/
NSLS II/FMX: https://www.bnl.gov/ps/beamlines/beamline.php?r=17-ID-2
SP8/BL32XU: http://www.spring8.or.jp/wkg/BL32XU/instrument/lang-en/INS-0000001513
NSRRC/TPS 07A: http://tpsbl.nsrrc.org.tw/bd_page.aspx?lang=en&port=07A&pid=1118
PETRA-III/P14: http://www.embl-hamburg.de/services/mx/P14/
SLS/X06SA: https://www.psi.ch/en/sls/pxi
DLS/ID24: https://www.diamond.ac.uk/Instruments/Mx/I24.html
ESRF/ID23-2: https://www.esrf.eu/UsersAndScience/Experiments/MX/About_our_beamlines/ID23-2

over, **TPS 07A** will be embedded with powerful software that automatically determines the results of the raster scan from a loop with many tiny crystals. A strategy of whether and how to collect those crystals will be provided. The ultimate objective is to provide an automatic workflow to make multi-crystal data collection even more efficient.

Since 2017 January, **TPS 05A** has been in full user operation. 72 user groups, comprising 68 academic user groups and four pharmaceutical companies, have collected diffraction data using this beamline. Until now, this beamline has produced 76 PDB depositions and 52 publications. Some of these results are highlighted below. One outstanding example in the evolutionary field is the structure of Asgard profiling (an ancient protein) in complex with Rabbit actin that has provided vital and critical clues to elucidate the possible origin of the eukaryotic cell.[1] Some examples in the immunology area are the complex structures of BTN3As (one of immune checkpoint proteins) with HMBPP (a potent microbial phosphoantigen) that have offered new strategies for the treatment of future T-cell immunotherapy[2] or the structures of echinomycin and Actinomycin D (two potent anticancer antibiotics) in complex with a DNA duplex containing a single T:T and G:G mismatch, respectively, that have illustrated the mechanism of how small-molecule ligands recognize these DNA mismatches and lead to potential applications in cancer diagnosis as well as the development of a novel therapeutic protocol.[3,4] Other examples in cell or DNA partitioning are the structures in the nuclear transport factor (Importin-α-GM130 complex) or in the partitioning system (*Hp*Soj-DNA complexes) that are required for chromosome or DNA maintenance during cell division.[5,6]

Regarding industrial applications, two such highlights are the structure of ZHD (a α-ZOL-hydrolyzing enzyme) in complex with α-ZOL (an estrogenic mycotoxin derivative) and the structure of PET (polyethylene terephthalate) hydrolase in complex with a PET analogue (HEMT). In the former case, α-ZOL is a major issue for farm animals and human beings; it hence causes significant economic loss. The structural information provides a key clue for a mycotoxin-biodegradation strategy. In the latter case, PET accounts for about 18% of the total plastic polymer in the world, so that PET is a large part of plastic pollution. According to the complex structure, it indicates that the enzymatic activity of PET hydrolase can be enhanced *via* protein engineering for future industrial application.[7,8]

In conclusion, **TPS 05A** is a workhorse for the crystallographic communities in Taiwan and other Asian countries, indicated by abundant structures deposited and high-impact papers published. In addition, with **TPS 07A** open to general users in 2022 January, the high-flux and special features of two TPS beamlines will be particularly useful for the most demanding crystallographic projects, such as those crystals with large unit cells (**TPS 05A**) and those with many tiny crystals (**TPS 07A**). (Reported by Chien-Chang Tseng and Chun-Hsiang Huang).

References

1. C. Akil, R. C. Robinson, Nature **562**, 439 (2018).
2. Y. Yang, L. Li, L. Yuan, X. Zhou, J. Duan, H. Xiao, N. Cai, S. Han, X. Ma, W. Liu, C. C. Chen, L. Wang, X. Li, J. Chen, N. Kang, J. Chen, Z. Shen, S. R. Malwal, W. Liu, Y. Shi, E. Oldfield, R. T. Guo, Y. Zhang, Immunity **50**, 1043 (2019).
3. P.-C. Wu, S.-L. Tzeng, C.-K. Chang, Y.-F. Kao, M. J. Waring, M.-H. Hou, Nucleic Acids Res. **46**, 7396 (2018).
4. R. Satange, C.-Y. Chuang, S. Neidle, M.-H. Hou, Nucleic Acids Res. **47**, 8899 (2019).
5. C.-C. Chang, C.-J. Chen, C. Grauffel, Y.-C. Pien, C. Lim, S.-Y. Tsai, K.-C. Hsia, Nat. Commun. **10**, 4307 (2019).
6. C.-H. Chu, C.-Y. Yen, B.-W. Chen, M.-G. Lin, L.-H. Wang, K.-Z. Tang, C.-D. Hsiao and Y.-J. Sun, Nucleic Acids Res. **47**, 2113 (2019).
7. Y. Zheng, W. Liu, C.-C. Chen, X. Hu, W. Liu, T.-P. Ko, X. Tang, H. Wei, J.-W. Huang, R.-T. Guo, ACS Catal. **8**, 4294 (2018).
8. X. Han, W. Liu, J.-W. Huang, J. Ma, Y. Zheng, T.-P. Ko, L. Xu, Y.-S. Cheng, C.-C. Chen, R.-T. Guo, Nat. Commun. **8**, 2106 (2017).

Advanced Micro-Crystal Chemical Crystallography

A beamline for micro-crystal X-ray diffraction (μ-XRD) is a dedicated beamline designed for advanced and non-ambient crystallography of chemical crystal research. This beamline, **TPS 15A**, is scheduled to be a Phase-II beamline at Taiwan Photon Source (TPS), and its construction began in 2019.

The layout of **TPS 15A** is shown in **Fig. 1**. It consists of a tapered cryogenic undulator source (CUT18) that will generate highly brilliant X-rays in designed energy range 9–35 keV. The photon flux of this energy range is 10^{13}–10^{14} photons/s (0.1% bw), shown in **Fig. 2**. X-ray beam modes of two types, monochromatic and pink beams, are selected with a coupled double-crystal monochromator (DCM)/double-multilayer monochromator (DMM) system. The energy bandwidth of the pink beam is designed to be 3 and 5% according to the multilayer coatings Pd/B_4C and W/B_4C, respectively. Three focusing mirrors (toroidal FM, VFM and HFM) are designed to focus the X-ray beam spot, first focused with the FM, then delivered to the VFM and then the HFM, down to diameter 10 x 10 μm² (FWHM). Two endstations (ES1 and ES2) will be installed; one locates after FM and another locates at the focused beam spot. The beam spot size is adjustable in the range 200 x 200–100 x 100 μm² at ES1 and 70 x 70–5 x 5 μm² at ES2. Experiments can be conducted in either monochromatic (with the DCM) or pink (with the DMM and selected bandwidth 3 or 5%) beam mode in both endstations. A home-built diffractometer will be installed at ES1; a highly precise microdiffractometer (MD3UP) and a large-area detector (EIGER 2X CdTe 9M) will be installed at ES2, shown in **Fig. 1(a)**.

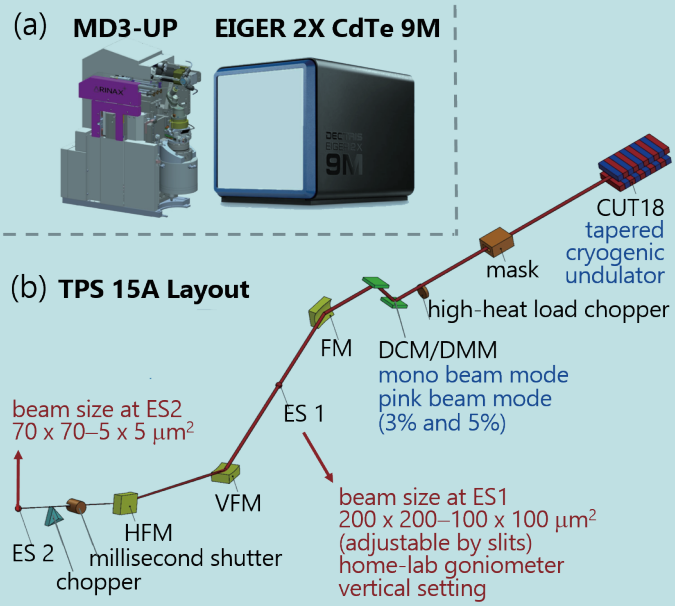

Fig. 1: (a) Microdiffractometer MD3UP and detector EIGER 2X CdTe 9M. (b) Layout of **TPS 15A**.

Single-crystal X-ray diffraction is a mature and routine technique that provides structural information from a single crystal. This information is important for the development of new materials through the relation with its physical and chemical properties. For example, graphite and diamond consist of carbon atoms, but their physical and chemical properties, such as shape, color, hardness *etc.*, differ markedly. Those differences can be explained by their structure–carbon atoms in graphite connect to each other with trigonal coordination, but in diamond all carbon atoms bind to each other with tetrahedral coordination.